QUANTITATIVE SURFACE ANALYSIS BY X-RAY PHOTOELECTRON SPECTROSCOPY

C.J. POWELL
National Bureau of Standards, Washington, D.C. 20234, USA

and

P.E. LARSON *
GCA/McPherson Instrument Corporation, 530 Main Street, Acton, Massachusetts 01720, USA

Received 11 July 1977

Measurements have been made of the relative intensities of the principal features in X-ray photoelectron spectra of indium, lead, and aluminum oxide and compared with those expected from a simple model for the photoemission process. Systematic effects in the determination of line intensities are discussed and a suitable procedure for determining intensities is described. The satisfactory agreement between computed and measured intensities confirms the validity and utility of the photoemission model and associated data, and indicates that quantitative analyses of homogeneous single–phase surfaces can be obtained by X-ray photoelectron spectroscopy.

1. Introduction

X-ray photoelectron spectroscopy (XPS) is now being widely applied for qualitative analyses of surfaces and there is considerable interest in making the technique more quantitative [1–11]. Three methods for quantitative analysis have been employed to date: local standards, elemental sensitivity factors, and use of a so-called first-principles model. Local standards are feasible only if samples with a limited range of compositions are to be routinely analyzed. Elemental sensitivity factors derived from measurements on a wide range of compounds [12–16] provide a relatively simple and rapid basis for surface analysis although neglect of the variation of electron attenuation lengths in different materials can lead to systematic errors. The first-principles model relates observed intensities to basic material properties and to the measurement conditions [17–29] but the application has been limited owing to uncertainty in the validity of the model (due to various approximations) or to lack of the necessary data.

* Present address: Hach Chemical Company, P.O. Box 389, Loveland, Colorado 80537, USA.

New data has become available recently for photoionization cross sections of specific subshells [30], electron attenuation lengths [31], and for observed XPS lineshapes [32]. The aim of the present paper is to test the validity of the first-principles model and the new data using XPS measurements made with several single-phase surfaces of known composition, the elements In and Pb, and the compound Al_2O_3. The elements In and Pb were selected for this test as they each have several XPS lines that can be excited by Mg Kα radiation, their electron energy-loss spectra have been previously measured and shown to consist predominantly of features due to plasmon excitation, the attenuation-length theory of Penn [31] should be applicable, and the asymmetry parameter for their XPS lineshapes had been measured [32]. The compound Al_2O_3 was selected as it was a simple compound that could be conveniently cleaned by sputtering.

2. Model and data

Certain assumptions and simplifying approximations are made in the model description of the XPS process [11,17]. We assume here that the sample is homogeneous and smooth (although both assumptions can be relaxed). The effects of elastic electron scattering are neglected as are possible anisotropies in electron transport in the sample. In essence, it is assumed that such effects are "averaged out" in a polycrystalline sample and that elastic scattering merely lengthens the average electron path in the sample by a constant fraction of the electron attenuation length in the sample [6,33]. Finally, it is assumed that reflection and refraction of X-rays and electrons at the sample–vacuum interface can be neglected and that the attenuation length for the incoming X-rays is much greater than the inelastic attenuation length for the outgoing electrons; these assumptions are reasonable for common conditions of XPS measurements.

With these assumptions, the measured current $I_s(E_{i,X})$ of photoelectrons of kinetic energy E_i excited from level X of the ith species in the sample s can be written in the form [11,17,34]

$$I_s(E_{i,X}) = I(\hbar\omega)N_i\sigma_i(\hbar\omega, \theta, X)\lambda_s(E_i)F(E_i, E_a)T(E_i, E_a)D(E)G \,. \quad (1)$$

In this equation, $I(\hbar\omega)$ is the X-ray flux incident on the sample at the characteristic energy $\hbar\omega$; N_i is the density of atoms of the ith species; $\sigma_i(\hbar\omega, \theta, X)$ is the photoionization cross section for the level X of the ith species at the X-ray energy $\hbar\omega$ and for the electron ejection angle θ; $\lambda_s(E_i)$ is the attenuation length in the sample for electrons of kinetic energy E_i; $F(E_i, E_a)$ is an electron-optical factor that may need to be included if electrons are decelerated from their initial energy E_i to some energy E_a before entering the energy analyzer; $T(E_i, E_a)$ is the transmission function of the analyzer and is defined in this form if E_a is a function of E_i; $D(E)$ is the efficiency of the detector for the electron energy E; and G is a geometrical factor that accounts for the area of the sample irradiated by X-rays and viewed by the analyzer.

The photoionization cross section in eq. (1) includes "final-state" or intrinsic processes (to be discussed below) and the current $I_s(E_{i,X})$ therefore includes photoelectrons with a range of kinetic energies in the vicinity of E_i.

Two parameters in eq. (1) depend on the properties of the sample, $\sigma_i(\hbar\omega, \theta, X)$ and $\lambda_s(E_i)$. Cross sections for photoionization are essentially [29,34] an atomic property, characteristic only of the ith species in the sample, whereas the attenuation length is a sample or matrix property that needs to be known for the kinetic energy E_i.

The desired cross section for photoionization is given by

$$\sigma_i(\hbar\omega, \theta, X) = \sigma_i(\hbar\omega, X)F(\theta, X, \hbar\omega)\, d\Omega/4\pi\,, \tag{2}$$

where $\sigma_i(\hbar\omega, X)$ is the total photoionization cross section (for all angles of photoejection), $F(\theta, X, \hbar\omega)$ is an angular asymmetry factor, and $d\Omega$ is the solid angle of acceptance of the analyzer, a constant for a particular instrument. Calculations of $\sigma_i(\hbar\omega, X)$ have been reported [30] for the Kα lines of Mg and Al and these are believed reliable as long as the X-ray energy is at least about 500 eV greater than the electron binding energy for the level X [35]. For $\theta = 90°$, a common experimental geometry, the angular asymmetry factor is given by [36]

$$F(90, X, \hbar\omega) = 1 + \beta(X, \hbar\omega)/4\,, \tag{3}$$

where $\beta(X, \hbar\omega)$ is the asymmetry parameter [36]. Values of $\beta(X, \hbar\omega)$ have been calculated recently by Reilman et al. [37] for the various levels X that can be excited by Mg and Al Kα radiation.

The electron attenuation length for $E_i \gtrsim 200$ eV can be expressed in the form

$$\lambda_s(E_i) = E_i/[a_s(\ln E_i + b_s)]\,, \tag{4}$$

where a_s and b_s are parameters characteristic of the sample. Penn [31] has computed values of a_s and b_s for free-electron-like elements (those for which the dominant inelastic scattering mechanism is plasmon excitation) and has estimated these parameters for other elements. For many situations, the assumption $b_s = -2.3$ can be a useful approximation [31].

Eqs. (1) to (4) can be used in two ways. First, one can compare XPS intensities $I_1(E_i)$ and $I_2(E_i)$ for the same excitation of a given atom in different compounds or alloys:

$$\frac{I_1(E_i)}{I_2(E_i)} = \frac{N_1\lambda_1(E_i)}{N_2\lambda_2(E_i)} \approx \frac{N_1 a_2}{N_2 a_1}\,. \tag{5}$$

That is, measured intensities can be used to obtain relative atomic concentrations if the electron attenuation lengths in the two samples are known. Second, one can compare XPS intensities $I_1(E_1)$ and $I_1(E_2)$ for excitations from different atoms in a single sample:

$$\frac{I_1(E_1)}{I_1(E_2)} = \frac{N_1\sigma_1\lambda_s(E_1)F(E_1,E_a)T(E_1,E_a)D(E_1)}{N_2\sigma_2\lambda_s(E_2)F(E_2,E_a)T(E_2,E_a)D(E_2)}$$

$$= \frac{N_1\sigma_1 E_1(\ln E_2 + b_s)F(E_1,E_a)T(E_1,E_a)D(E_1)}{N_2\sigma_2 E_2(\ln E_1 + b_s)F(E_2,E_a)T(E_2,E_a)D(E_2)}. \quad (6)$$

Absolute values of attenuation lengths are not required with eq. (6) but knowledge is needed instead of the photoionization cross sections and the instrumental parameters. Eq. (6) will be used in the following analysis.

3. Intensity measurements

A satisfactory surface analysis by XPS requires a separation of that intensity corresponding to $\sigma_i(\hbar\omega, \theta, X)$ in eq. (1) from other features in experimental XPS data [34]. Fig. 1 shows an XPS spectrum for the favorable case where the most prominent feature is a relatively sharp peak and where features to lower kinetic energy can be associated with single surface and bulk plasmon excitation of the emerging photoelectrons. Determination of the desired XPS intensity requires consideration of the background under the peak, the intensity due to inelastic scattering ("extrinsic" processes), the intensity due to shakeup or final-state effects ("intrinsic" processes), and the lineshape of the parent XPS line; the role of these factors in the intensity measurement will now be discussed in turn.

Features in the observed spectrum appear, in general, on a continuous background due to multiple inelastic scattering of photoelectrons of initially higher ki-

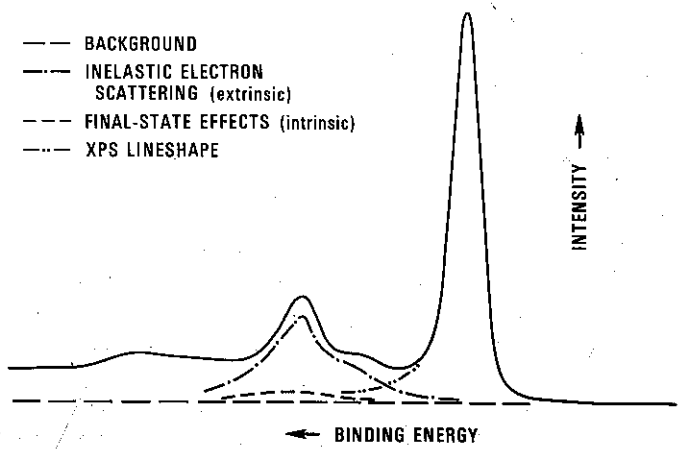

Fig. 1. Schematic diagram of an observed XPS line (solid line). The other lines represent estimates of the separate contributions of the background, inelastic electron scattering, final-state effects, and of the XPS lineshape, as described in the text.

netic energy and to photoemission caused by bremsstrahlung from the X-ray source. The background under the peak can therefore be found by simple analytic extrapolation from high to low kinetic energies, as represented by the long-dashed line in fig. 1. This procedure is believed to be adequate for the extrapolations of 10 to 20 eV performed here.

The dot-dashed line in fig. 1 is an approximate representation of the intensity due to electrons which have suffered *single* inelastic electron scattering. The principal features of such extrinsic processes should appear as "daughters" on all observed "parent" XPS lines and should correspond to separate measurements of energy loss spectra measured when electron beams interact with solid targets [38]. The intensity of the feature due to surface-plasmon excitation relative to that due to bulk-plasmon excitation will get larger as the electron energy becomes smaller, as the angle between the photoelectron direction and the surface becomes smaller, and as the surface becomes smoother [38,39]. The combined intensity of the bulk- and surface-plasmon excitations, however, should be approximately equal to the intensity of the parent XPS line [40–42].

The short-dashed line in fig. 1 is an approximate indication of the intensity due to the intrinsic excitation of bulk plasmons in the photoionization process; some additional intensity due to intrinsic surface-plasmon excitation is also possible. There is, at present, some controversy over the relative magnitude of intrinsic and extrinsic processes [43] and there is some reason to believe that a precise separation of intrinsic and extrinsic processes is not possible [44]. A well-established sum rule [45] indicates that the intensity due to intrinsic plasmon excitation should amount to about 30% of the intensity of the parent line [46]. Gadzuk [47], however, has shown that for the photoelectron energies normally encountered in XPS the sudden approximation [6] breaks down and the intrinsic intensity should be about half of the estimates made on the basis of this approximation.

Finally, the dashed-double-dot line in fig. 1 represents the line shape of the parent XPS feature of the following form [48]:

$$I(\epsilon) = \frac{\cos[\frac{1}{2}\pi\alpha + (1-\alpha)\arctan\epsilon/\gamma]}{[\epsilon^2+\gamma^2]^{(1-\alpha)/2}} \quad (7)$$

In eq. (7), $I(\epsilon)$ is the intensity of the line as a function of energy, 2γ is the natural width (full width at half-maximum intensity) of the core level due to lifetime broadening, and α is an asymmetry parameter. Values of α have been determined [32] to lie in the range 0 to 0.3 (being zero for insulators and large for metals with a high density of states at the Fermi level). Eq. (7) is believed to be valid for $|\epsilon|$ less than the Fermi energy [49] but unfortunately eq. (7) cannot be integrated to provide a finite area for the total line intensity [32]. Also, the measured line shape will be distorted in the vicinity of the peak by broadening contributions from the X-ray source and the electron energy analyzer although eq. (7) can be used to give the line shape for the nearby wings of the line.

The foregoing discussion indicates that it is not possible to determine unambiguously the intensity corresponding to $\sigma_i(\hbar\omega, \theta, X)$ in eq. (1) of a line in XPS data. We now describe two procedures which we have used to obtain approximate measures of XPS intensities. In each case we have made a measurement of part of the desired XPS intensity in order to avoid the considerable uncertainties associated with decomposing the observed spectrum into its separate components. Both procedures have been designed to make maximum use of the physical constraints noted above.

For the first procedure, procedure A, we have chosen to integrate each XPS line between two limits symmetrically located about the line center, as represented by the vertical lines A in fig. 2. The separation in energy between the lower limit and the line center, in this case 5 eV, should be selected to be close to the intensity minimum that exists for most actual XPS data between the parent line and the structure due to intrinsic- and extrinsic-plasmon excitation. For many materials, the bulk-plasmon energy is usually between 10 and 25 eV, so that a lower limit between about 5 and 10 eV from the line center would be appropriate. We can in this way minimize the uncertainty associated with the lack of detailed knowledge of the intrinsic-plasmon intensity and of the intensity in the tail extending to lower kinetic energies. Our intention here is to try to discard a nearly constant fraction of the total intensity [given by eq. (7)] outside the limits A (for each XPS line from a sample) and so to eliminate the practical difficulty of measuring the intensity in the tails of the line and our inability to determine a correction factor from eq. (7) for this intensity. In essence, we make use of the fact that the parameter α should be a constant for all XPS lines from a sample.

This procedure has two principal sources of error. First, it is not known, a priori, that the intensity of the shakeup satellites will necessarily be the same for all XPS

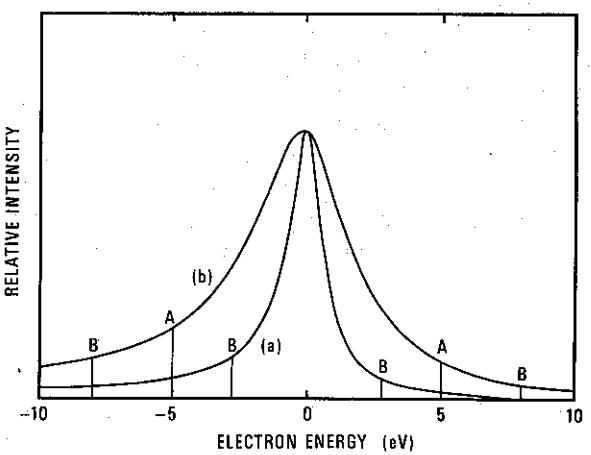

Fig. 2. Plots of eq. (7) with $\alpha = 0.11$ for (a) $\gamma = 0.7$ eV and (b) $\gamma = 2$ eV to show the effects of fixed limits of integration of 5 eV (procedure A) and of integration limits of $\pm 4\gamma$ (procedure B) on measurements of XPS intensities for lines of different natural widths.

lines from a sample. For the special case of intrinsic-plasmon excitation, it is a reasonable approximation so long as the photoelectron leaves the atom at a sufficiently high velocity that the sudden approximation [6] is valid. It has been shown, however, that the fraction of the total line intensity due to intrinsic-plasmon excitation should be a function of photoelectron energy in the range of interest [47]; if, however, this fractional intensity is small (say less than 15%), the variation of this fraction with photoelectron energy need not be a serious source of error. Alternatively, a suitable correction factor can be applied to the measured areas. For XPS data where intrinsic-plasmon excitation is not believed to be the dominant final-state effect, a comparison can be made of the structure on the low-kinetic-energy side of different parent peaks for a given sample. Obvious variations in the relative intensities of this satellite structure would be an indication that the fraction of intensity in the shake-up satellites was different for different XPS lines.

A second source of error not accounted for is the fact that different XPS lines from a sample will, in general, have different half widths (values of γ). If typical values of γ were much less than the limits of integration defined above, a negligible fraction of the intensity in the lorentzian tails of the line would be discarded and there would be little error. If γ is comparable to the integration limits, the error becomes significant. In practice, however, the stronger, sharper XPS lines are usually measured rather than the weaker, broader lines.

For the second procedure, procedure B, limits of integration are indicated by the lines B in fig. 2. Each limit has been set at a constant multiple of the value of γ for each line. Limits of $\pm 4\gamma$ are chosen for illustration here so that a reasonably large fraction of the line intensity in the tails is included in the integration. If much smaller limits are selected, an explicit correction for the instrument response function would become necessary. If the limits are much larger, the uncertainty in background location at the lower kinetic energies becomes an important source of error.

Procedure B also is subject to the first source of error noted above for procedure A but overcomes the second source of error. By setting the integration limits as a function of γ, we can measure the same fraction of the total intensity for each XPS line in a given sample [32]. The accuracy of the procedure will then depend on the extent to which the parameter α is known for the sample and the extent to which the half widths γ are known for different lines [50] (or can be determined from the experimental data after deconvolution of the instrument response function).

4. Experimental

The X-ray photoelectron spectra were obtained with a McPherson ESCA 36 electron spectrometer * for which there is no deceleration of the photoelectrons before

* Commercial equipment is identified here in order to specify the experimental conditions. This identification does not imply recommendation or endorsement by the National Bureau of Standards nor does it imply that this equipment is necessarily the best available for the purpose.

energy analysis [$E_i = E_a$ in eq. (1)]. The transmission function of the spherical-deflector energy analyzer is known from first principles to be a linear function of electron energy [51]. That is, for eq. (1),

$$F(E_i, E_i) = 1 , \tag{8a}$$

and

$$T(E_i) = A\, E_i , \tag{8b}$$

where A is an instrumental constant.

The electron detector in this instrument is a channel electron multiplier; according to the manufacturer, there should be negligible variation in detector efficiency with photoelectron energy in the range of interest here. That is,

$$D(E) = B , \tag{8c}$$

where B is a constant.

XPS data for each sample were obtained after sputtering with argon ions until the intensity of features due to initial surface contaminants (carbon and oxygen) was negligible (<2% of the intensity of major features). The argon 2p signal was less than 1% of the In $3d_{5/2}$ signal and of the Pb $4f_{7/2}$ signal but was about 15% of the O 1s signal in Al_2O_3. For each sample, the energy-loss features were similar to those that have been observed in independent experiments: surface- and bulk-plasmon energies of 8.7 eV and 11.3 eV, respectively, in indium [52]; surface- and bulk-plasmon energies of 10.6 eV and 13.9 eV, respectively, in lead [53]; and a bulk-plasmon energy of about 23 eV in aluminum oxide [54].

5. Results

Figs. 3–5 show XPS data for the most intense lines observed for each sample. The 4p level of In was not analyzed as this lineshape is known not to be represented by eq. (7) for In and neighboring elements in the periodic table [55]. We chose to analyze the component of smaller binding energy for certain spin–orbit-split doublets (3d of In, and 5d, 4f, and 4d of Pb) because of uncertainty in background location for the other component.

The spectra shown in figs. 3–5 are those obtained after the intensity due to the Mg $K\alpha_{3,4}$ satellite was removed (by subtracting from the observed data a constant fraction of the structure excited by the Mg $K\alpha_{1,2}$ radiation). The data was acquired in digital form and figs. 3–5 show smooth curves drawn through the data points after a fixed number of counts, constant for each XPS line, was subtracted from the data. The ordinates in figs. 3–5 represent difference intensities with a common scale for each material.

The long-dashed lines in figs. 3–5 represent backgrounds under the peaks of interest estimated using the criteria described above. Use also was made of XPS data

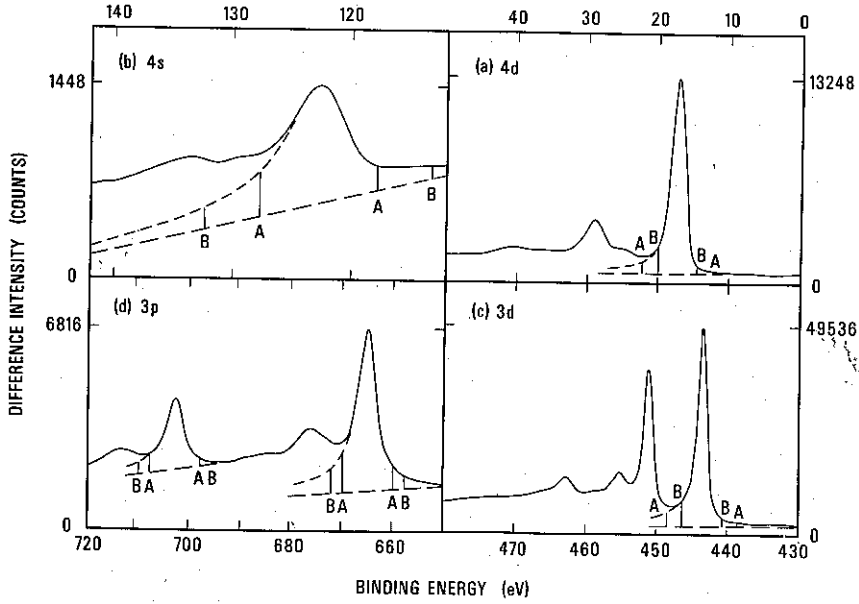

Fig. 3. XPS data for indium (note different energy scales in separate panels).

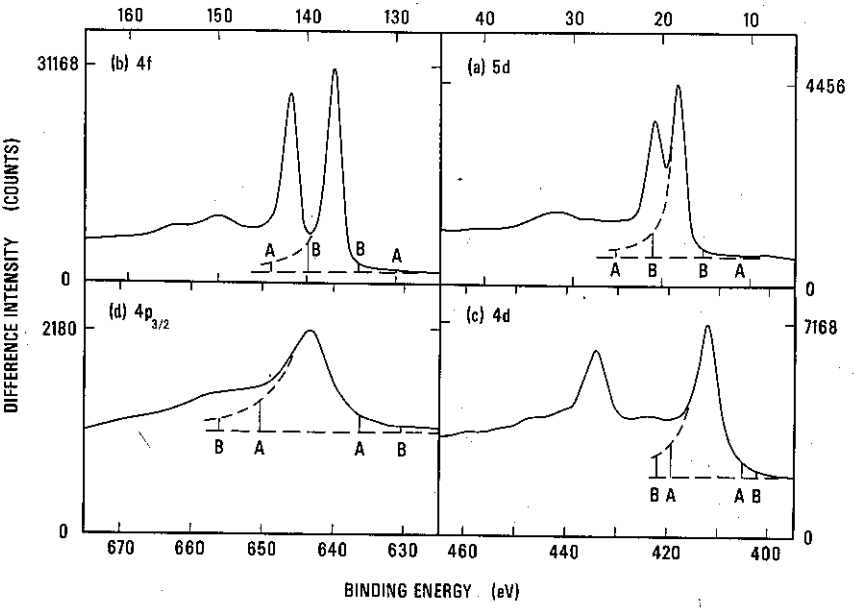

Fig. 4. XPS data for lead (note different energy scales in separate panels).

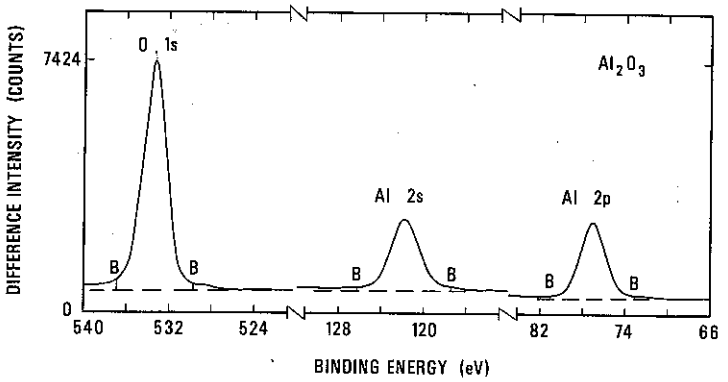

Fig. 5. XPS data for aluminum oxide.

from 0 to 1000 eV binding energy. The short-dashed line is a fit of eq. (7) to the tails of each line. The parameter α has been determined for In to be 0.11 ± 0.01 by Hufner et al. [56] and γ was then used as an adjustable parameter to fit the observed line profile. We did not resolve the In 4d and Al 2p spin–orbit-split doublets and the values of γ derived for the composite peaks have little direct significance; we did, however, use these "effective" values of γ in setting integration limits for these peaks by procedure B. No measurements of α for lead were found and we have used the value $\alpha = 0.11$ based on measurements for the similar metals tin and indium. The parameter α is known to be zero for the insulator Al_2O_3.

Vertical lines in figs. 3–5 show the integration limits for the determination of peak areas by procedures A and B. We chose integration limits of ±5 eV and ±7 eV for In and Pb, respectively, based on the criteria discussed above for intensity measurements by procedure A. Integration limits of ±4γ were set for In, Pb, and Al_2O_3 for intensity measurement by procedure B. Areas under each peak were measured with a planimeter.

Tables 1 and 2 show the relative peak areas determined using procedures A and B. We also show the predicted relative intensities on the basis of eqs. (2), (3), (6) and (8), namely

$$I_s(E_{i,X}) = \frac{CN_i\sigma_i(\hbar\omega, X)(1 + \beta(X, \hbar\omega)/4)E_i^2}{(\ln E_i + b_s)}, \tag{9}$$

where C is a constant. We also show in tables 1–3 the values of $\sigma_i(\hbar\omega, X)$ (given relative to the cross section for photoionization of the carbon 1s level) calculated by Scofield [30] and the values of β calculated by Reilman et al. [37] which we have used in calculating relative intensities (tables 1 and 2) or in deriving relative atomic concentrations (table 3). We have used the values of b_s calculated by Penn [31] of −1.80, −1.97, and −2.79 for In, Pb, and Al_2O_3, respectively.

Table 1
Measured and predicted XPS relative intensities for selected XPS peaks of In excited by Mg Kα radiation. The measured intensities were obtained by the procedures A and B described in the text; for procedure B, the indicated values of γ were used. The predicted intensities were obtained with the use of eq. (9) and the indicated parameters

	Level				
	4d	4s	$3d_{5/2}$	$3p_{3/2}$	$3p_{1/2}$
Photoelectron energy (eV)	1236.4	1130.6	810.1	588.7	551
γ (eV)	0.7	2.4	0.6	1.8	1.8
Procedure A (integration limits of ±5 eV) measured relative intensities	0.34	0.05	1	0.26	0.11
Procedure B (integration limits of ±4γ) measured relative intensities	0.35	0.08	1	0.34	0.14
Predicted intensities [eq. (9)]					
$\sigma_i(\hbar\omega, X)$ (ref. [30])	2.183	0.611	13.23	7.27	3.51
$\beta(X, \hbar\omega)$ (ref. [37])	1.30	2	1.18	1.54	1.54
Computed relative intensities	0.36	0.10	1	0.33	0.14

Table 2
Measured and predicted XPS relative intensities for selected XPS peaks of Pb excited by Mg Kα radiation. The measured intensities were obtained by the procedures A and B described in the text; for procedure B, the indicated values of γ were used. The predicted intensities were obtained with the use of eq. (9) and the indicated parameters

	Level			
	$5d_{5/2}$	$4f_{7/2}$	$4d_{5/2}$	$4p_{3/2}$
Photoelectron energy (eV)	1235.4	1116.6	841.4	610.4
γ (eV)	0.7	0.7	2.5	3.2
Procedure A (integration limits of ±7 eV) measured relative intensities	0.13	1	0.43	0.11
Procedure B (integration limits of ±4γ) measured relative intensities	0.13	1	0.57	0.16
Predicted intensities [eq. (9)]				
$\sigma_i(\hbar\omega, X)$ (ref. [30])	1.29	12.83	10.37	4.86
$\beta(X, \hbar\omega)$ (ref. [37])	1.32	0.98	1.11	1.51
Computed relative intensities	0.13	1	0.50	0.14

Table 3
Relative intensities (measured with procedure B) of XPS lines for sputtered aluminum oxide with Mg Kα radiation and derived relative atomic concentrations of aluminum and oxygen with the use of eq. (9)

	Level		
	O 1s	Al 2s	Al 2p
Photoelectron energy (eV)	720.3	1131.8	1176.6
γ (eV)	0.9	1.1	1.0
Measured relative intensities	1	0.39	0.35
$\sigma_i(\hbar\omega, X)$ (ref. [30])	2.85	0.681	0.574
$\beta(X, \hbar\omega)$ (ref. [37])	2	2	1.025
Relative aluminum and oxygen atomic concentrations			
(a) using O 1s and Al 2s signals	1.35	1	
(b) using O 1s and Al 2p signals	1.13		1

6. Discussion

It is clear from figs. 3 and 4 that procedures A and B measure different fractions of the total XPS intensity for lines of different half width. Tables 1 and 2 show that the relative intensities determined by procedure B agree much better with intensities computed from eq. (9) than those obtained with procedure A. This result is considered reasonable as procedure B enables an essentially constant fraction of the total intensity of each line to be measured.

The high degree of consistency that has been obtained between experimental relative intensities from procedure B and predicted relative intensities from eq. (9) for In and Pb indicates that the model description on which eq. (9) is based is a satisfactory description of XPS for at least these two metals, that the calculated values of $\sigma_i(\hbar\omega, X)$ and $\beta(X, \hbar\omega)$ provide an adequate description of photoionization cross sections [30,37], that eq. (4) gives a satisfactory variation of the electron attenuation length with energy [31], and that useful measurements of XPS intensities can be made with procedure B. Although further work is required to determine whether a similar high degree of consistency can be obtained with other elements, we believe that this will be likely based on the degree of success which has been obtained in previous measurements and comparisons of this type [12–15,21,24,27,28]. We believe that we have obtained better consistency between theoretical and experimental XPS intensities than in these earlier comparisons because we have made a

more accurate measurement of the XPS intensities, have taken the systematic effects of angular asymmetry in photoionization from different shells into account [eq. (3)], have used a more accurate equation for the variation of electron attenuation length with kinetic energy [eq. (4)], and have used an electron spectrometer for which the transmission function [eq. (8b)] is well established.

The utility of XPS for quantitative surface analysis is dependent on a number of physical factors [34], one of which is the ability to make meaningful measurements of XPS intensities. We have been fortunate that eq. (7) has been tested and the parameter α determined for a number of metals [32,56]. It is clear that proper account needs to be taken of the expected asymmetry of XPS lines, particularly in measurements made with transition metals and their alloys [32]. Care also has to be taken in the determination of peak areas by procedure B when the observed lineshape is largely determined by the instrumental resolution and when an expected multiplet is not resolved.

Table 3 shows results of the XPS measurements on sputtered aluminum oxide for which intensities were measured with procedure B. Use of eq. (9) with the oxygen 1s and the aluminum 2s or 2p intensities yielded two measurements of the relative atomic concentrations of aluminum and oxygen which were different. A systematic effect of this type has been reported previously [27,28,57] and does not seem to be adequately accounted for by the calculated photoionization cross sections. Values of the Al 2s and 2p photoionization cross sections (for Mg Kα radiation) obtained by Scofield [30] and by Nefedov et al. [15] are identical but use of the calculated cross sections of Chapman and Lohr [58] increases slightly the difference in the Al concentrations obtained from the Al 2s and 2p intensities. Our estimate of the Al 2p intensity is an overestimate in that we have not resolved the spin–orbit-split 2p doublet and determined the correct (smaller) value of γ to use in the intensity measurement by procedure B. We do not believe, however, that this factor provides a complete explanation for the different Al concentrations derived from the 2s and 2p intensities.

Owing to the uncertainty in the determination of the Al 2p intensity, we use the Al 2s intensity to obtain a ratio of the aluminum atomic concentration to the oxygen atomic concentration of 2:2.7. This ratio is slightly different from the expected ratio of 2:3 but the difference may not be significant on account of the uncertainty in intensity measurements (estimated to be about ±5%), uncertainties in the ratios of cross sections (estimated to be about ±5%), and to the presence of some implanted argon in the sample.

7. Conclusion

We have reported measurements of the principal features in the X-ray photoelectron spectra of indium and lead excited by Mg Kα radiation. Relative intensities of these features were determined by two methods, one in which the limits of integra-

tion were set at the same value for each feature in the spectrum (procedure A) and one in which the limits of integration were set at a constant multiple of the line width (procedure B). Procedure B was judged to be the most satisfactory in that the same constant fraction of the total intensity for each line could be measured. Measurements of the relative line intensities for In and Pb by procedure B were also found to agree well with the values expected on the basis of a simple model for the XPS process. We were thus able to test simultaneously the validity and practical utility of the XPS model, recent calculations of photoionization cross-section data [30,37], the energy variation of the electron attenuation length in the sample [31], and data concerning the XPS lineshape [32,48].

We have used procedure B to measure relative intensities of the XPS features for sputtered aluminum oxide. A small systematic discrepancy was noted in the relative atomic concentration of Al determined from the Al 2s and 2p intensities; part of this discrepancy was associated with uncertainty in the determination of the correct relative Al 2p intensity. Use of the Al 2s and the O 1s intensities yielded relative atomic concentrations of Al and O in the ratio 2:2.7, a result judged sufficiently close to the expected ratio of 2:3.

We have taken account of known systematic effects in X-ray photoelectron spectroscopy and have obtained better agreement between predicted and measured intensities than in similar previous investigations [12–15,21,24,27,28]. Although simplifying assumptions have been made in obtaining eq. (1) which predicts XPS intensities, the level of agreement between computed and observed intensities obtained here and in earlier measurements indicates that XPS can be used for the quantitative analysis of homogeneous single-phase solid surfaces. Further work, however, is needed to establish the accuracy of measurement for different elements and compounds and, particularly, to determine the fraction of the total XPS intensity which goes into final-state or intrinsic satellites.

Acknowledgment

The authors are indebted to Dr. J.W. Gadzuk for discussions and insight concerning many-body effects on XPS lineshapes.

References

[1] S.H. Hercules and D.M. Hercules, in: Characterization of Solid Surfaces, eds. P.F. Kane and G.B. Larrabee (Plenum Press, New York, 1974) p. 307.
[2] W.M. Riggs and M.J. Parker, in: Methods of Surface Analysis, ed. A.W. Czanderna (Elsevier, New York, 1975) p. 103.
[3] K.L. Cheng and J.W. Prather, CRC Crit. Rev. Anal. Chem. 5 (1975) 37.
[4] R.S. Swingle and W.M. Riggs, CRC Crit. Rev. Anal. Chem. 5 (1975) 267.
[5] K. Siegbahn, J. Electron Spectry. 5 (1974) 307.

[6] T.A. Carlson, Photoelectron and Auger Spectroscopy (Plenum Press, New York, 1975).
[7] H.K. Herglotz and H.L. Suchan, Adv. Colloid Interface Sci. 5 (1975) 79.
[8] J. Tousset, Analusis 3 (1975) 221.
[9] D. Brion and J. Escard, J. Microsc. Spectrosc. Electr. 1 (1976) 227.
[10] D. Berenyi, in: Advances in Electronics and Electron Physics, ed. L. Marton (Academic Press, New York, 1976) p. 55.
[11] C.S. Fadley, in: Progress in Solid State Chemistry, eds. G. Somorjai and J. McCaldin (Pergamon Press, New York, 1976) p. 265.
[12] C.D. Wagner, Anal. Chem. 44 (1972) 1050.
[13] C.K. Jorgensen and H. Berthou, Faraday Disc. Chem. Soc. 54 (1973) 269.
[14] H. Berthou and C.K. Jorgensen, Anal. Chem. 47 (1975) 482.
[15] V.I. Nefedov, N.P. Sergushin, I.M. Band and M.B. Trzhaskovskaya, J. Electron Spectry. 2 (1973) 383.
[16] V.I. Nefedov, N.P. Sergushin, Y.V. Salyn, I.M. Band and M.B. Trzhaskovskaya, J. Electron Spectry. 7 (1975) 175.
[17] B.L. Henke, Phys. Rev. A 6 (1972) 94.
[18] P.E. Larson, Anal. Chem. 44 (1972) 1678.
[19] H. Ebel and M.F. Ebel, X-ray Spectrom. 2 (1973) 19.
[20] M.F. Ebel, J. Electron Spectry. 5 (1974) 837.
[21] W.J. Carter, G.K. Schweitzer and T.A. Carlson, J. Electron Spectry. 5 (1974) 827.
[22] C.S. Fadley, R.J. Baird, W. Siekhaus, T. Novakov and S.A.L. Bergstrom, J. Electron Spectry. 4 (1974) 93.
[23] D.M. Wyatt, J.C. Carver and D.M. Hercules, Anal. Chem. 47 (1975) 1297.
[24] M. Janghorbani, M. Vulli and J. Starke, Anal. Chem. 47 (1975) 2200.
[25] R.S. Swingle, Anal. Chem. 47 (1975) 21.
[26] K.T. Ng and D.M. Hercules, J. Electron Spectry. 7 (1975) 257.
[27] R.C.G. Leckey, Phys. Rev. A 13 (1976) 1043.
[28] L.J. Brillson and G.P. Ceasar, Surface Sci. 58 (1976) 457.
[29] C.D. Wagner, Anal. Chem. 49 (1977) 1282;
S. Evans, R.G. Pritchard and J.M. Thomas, J. Phys. C 10 (1977) 2485.
[30] J.H. Scofield, J. Electron Spectry. 8 (1976) 129.
[31] D.R. Penn, J. Electron Spectry. 9 (1976) 29.
[32] G. Wertheim and S. Hufner, J. Inorg. Nucl. Chem. 38 (1976) 1701.
[33] C.J. Powell, Surface Sci. 44 (1974) 29.
[34] C.J. Powell, in: Quantitative Surface Analysis of Materials, ed. N.S. McIntyre, ASTM STP 643 (American Society for Testing and Materials, Philadelphia, 1978) in press.
[35] J.W. Cooper, in: Atomic Inner-Shell Processes, Vol. 1, ed. B. Crasemann (Academic Press, New York, 1975) p. 159.
[36] D.J. Kennedy and S.T. Manson, Phys. Rev. A 5 (1972) 227.
[37] R.F. Reilman, A. Msezane and S.T. Manson, J. Electron Spectry. 8 (1976) 389.
[38] H. Raether, Springer Tracts Mod. Phys. 38 (1965) 84;
J. Daniels, C. von Festenburg, H. Raether and K. Zeppenfeld, Springer Tracts Mod. Phys. 54 (1970) 77.
[39] C.J. Powell, Phys. Rev. 175 (1968) 972.
[40] G.D. Mahan, Phys. Status Solidi (b) 55 (1973) 703.
[41] P.J. Feibelman, Surface Sci. 36 (1973) 558.
[42] M. Sunjic and D. Sokcevic, J. Electron Spectry. 5 (1974) 963.
[43] J.C. Fuggle, D.J. Fabian and L.M. Watson, J. Electron Spectry. 9 (1976) 99.
[44] M. Sunjic and D. Sokcevic, Solid State Commun. 18 (1976) 373.
[45] B.I. Lundqvist, Phys. Kondens. Mater. 9 (1969) 236;
R. Manne and T. Aberg, Chem. Phys. Letters 7 (1970) 282.

[46] J.W. Gadzuk, in: Photoemission from Surfaces, eds. B. Feuerbacher, B. Fitton and R.F. Willis (Wiley, New York), to be published.
[47] J.W. Gadzuk, J. Electron Spectry. 11 (1977) 355.
[48] S. Doniach and M. Sunjic, J. Phys. C 3 (1970) 285.
[49] P. Minnhagen, Phys. Lett. 56A (1976) 327.
[50] O. Keski-Rahkonen and M.O. Krause, At. Data Nucl. Data Tables 14 (1974) 139.
[51] C.E. Kuyatt, in: Methods of Experimental Physics, Vol. 7A, ed. L. Marton (Academic Press, New York, 1968) p. 16.
[52] J.L. Robins, Proc. Phys. Soc. (London) 79 (1962) 119.
[53] C.J. Powell, Proc. Phys. Soc. (London) 76 (1960) 593.
[54] N. Swanson, Phys. Rev. 165 (1968) 1067.
[55] G.B. Fisher, Bull. Am. Phys. Soc. 19 (1974) 233;
U. Gelius, J. Electron Spectry. 5 (1974) 985;
S.P. Kowalczyk, L. Ley, R.L. Martin, F.R. McFreely and D.A. Shirley, Faraday Discuss. Chem. Soc. no. 60 (1975) 7;
M.H. Chen, B. Crasemann, L.I. Yin, T. Tsang and I. Adler, Phys. Rev. A 13 (1976) 1435.
[56] S. Hufner, G.K. Wertheim and J.H. Wernick, Solid State Commun. 17 (1975) 417.
[57] U. Gelius, in: Electron Spectroscopy, ed. D.A. Shirley (North-Holland, Amsterdam, 1972) p. 311.
[58] F.M. Chapman and L.L. Lohr, J. Am. Chem. Soc. 96 (1974) 4731.